the total weekly trip frequency had to be increased to 860, requiring a total of 4033 block hours. The average load factor decreased from 0.4649 to 0.4595. The increase in block hours caused the total aircraft investment price to increase by $32,000,000.

Customarily, depreciation is included as part of operating cost. This has not been done here. AEDE treats investment cost more realistically by converting net weekly profit to present value of gross weekly profit over y years and $i\%$ interest on money. The result is compared with total present dollars invested in aircraft.

The net impact of lowering $W^*(T)$ can be visualized by comparing figures of merit; e.g., the present value of profit per dollar invested in aircraft decreases from $2.16 to $2.04 (Table 4). Other figures of merit are available to the AEDE user, e.g., net profit present value, present value of gross profit, or total annual cost.

In conclusion, AEDE provides a fair economic comparison between competing aircraft over the same route system. Its use can be extended to provide sensitivities to changes to aircraft performance, aircraft sizing, route system modification, changes in economic variables, and turnaround times and through stop capability.

Reference

[1] Lloyd-Jones, D. J., "Airline Equipment Planning, AAIA Paper 67-392, Los Angeles, Calif., 1967.

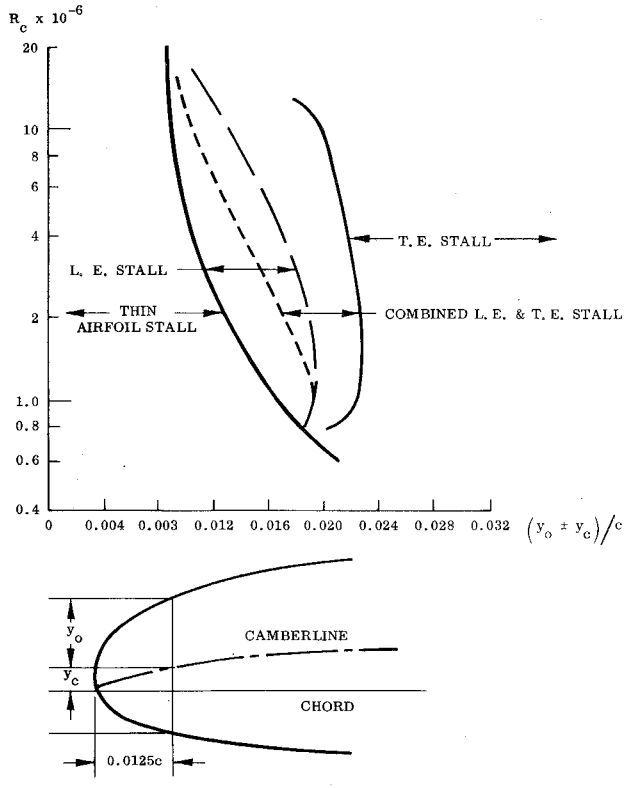

Fig. 1 Reynolds number airfoil thickness map for transition between stall types (Ref. 4).

Dynamic Stall Simulation Problems

LARS E. ERICSSON* AND J. PETER REDING†
Lockheed Missiles and Space Company, Sunnyvale, Calif.

DYNAMIC airfoil stall is a problem of concern both to compressor and helicopter industry. The problem has so far defied theoretical solution, and the only recourse has been simulation of dynamic stall in ground facilities, such as wind tunnels. Already static airfoil stall is difficult to simulate due to wind-tunnel wall and support interference, and the sensitivity of stall to surface roughness, Reynolds number, and wind-tunnel turbulence. This is at least true for trailing-edge and leading-edge stall, the two stall types of practical interest for the relatively thick airfoils used for compressor and helicopter blades. In the dynamic case, there are additional simulation problems associated with the effects of the airfoil oscillation on the effective adversity of the pressure gradient and the effective air turbulence (or Reynolds number).

It can be shown that the measured undamping at stall is caused by the pitch-rate induced accelerated flow effect and resultant delay of separation and reattachment.[1] The accelerating flow on the leeward side of a pitching airfoil causes a decrease in the adversity of the pressure gradient, resulting in a large overshoot of the static stall.[2] A similar lessening of the adversity of the pressure gradient can be accomplished by "nose droop," also resulting in an overshoot of the stall.[3] That is, the pitch rate induces a change of the effective airfoil shape.

Gault[4] has shown that the stall type is determined by the Reynolds number and a profile coordinate that effectively is a measure of the leading-edge curvature (Fig. 1). The figure is very instructive and demonstrates that it will take very little change in camber to convert leading-edge stall to trailing-edge

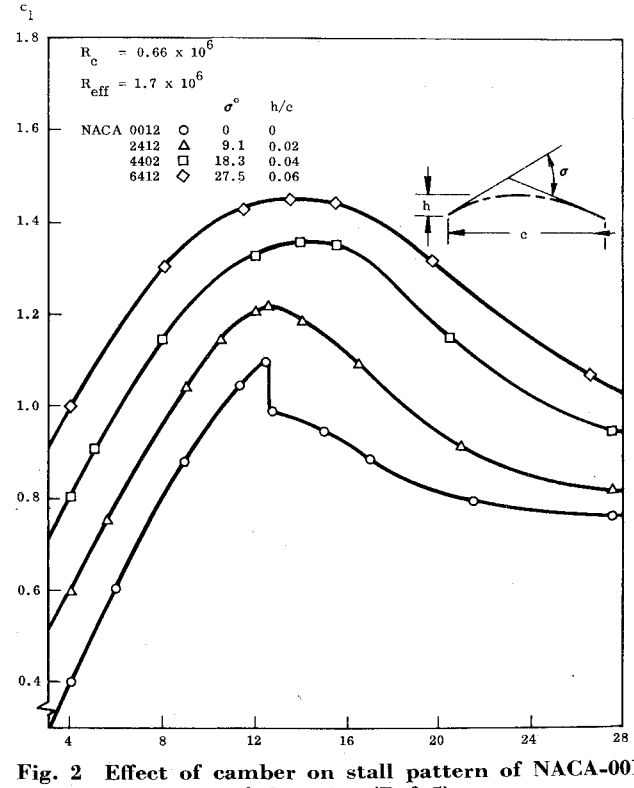

Fig. 2 Effect of camber on stall pattern of NACA-0012 airfoil section (Ref. 5).

Presented as Paper 70-945 at the AIAA Guidance, Control and Flight Mechanics Conference, Santa Barbara, Calif., August 17–19, 1970; submitted August 24, 1970; revision received April 19, 1971. The results were obtained in a study made for NASA Langley Research Center, Contract NAS 1-7999, under the direction of P. Hanson.

Index Category: Nonsteady Aerodynamics; Airplane and Component Aerodynamics.

* Senior Staff Engineer. Associate Fellow AIAA.

† Research Specialist. Member AIAA.

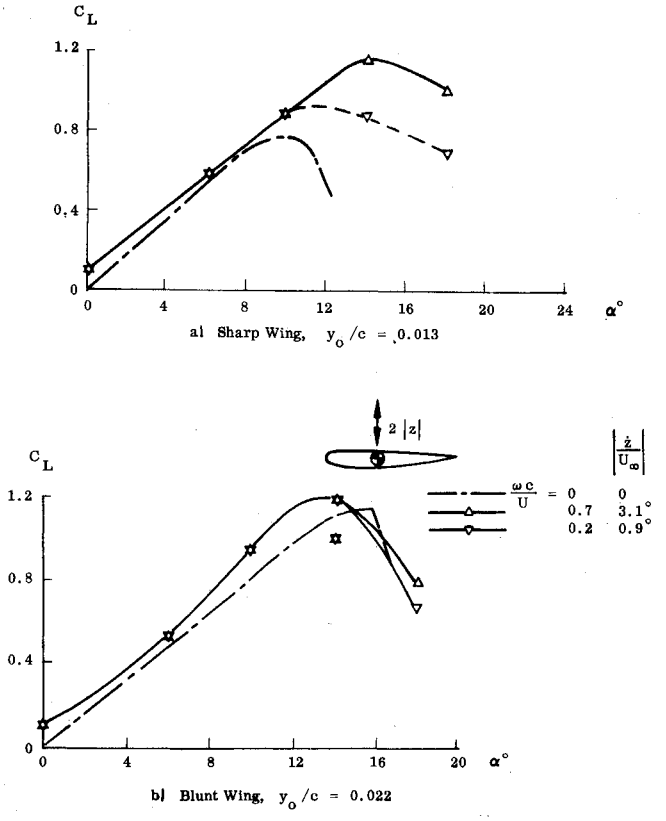

Fig. 3 Time average $C_L(\alpha)$-curves for translation at R_c = 10^6 (Ref. 7).

stall, and vice versa, if the camber and thickness combine to give values of the geometric correlation parameter in the range $0.01 < (y_0 + y_c)/c < 0.02$. The popular NACA 0012 airfoil

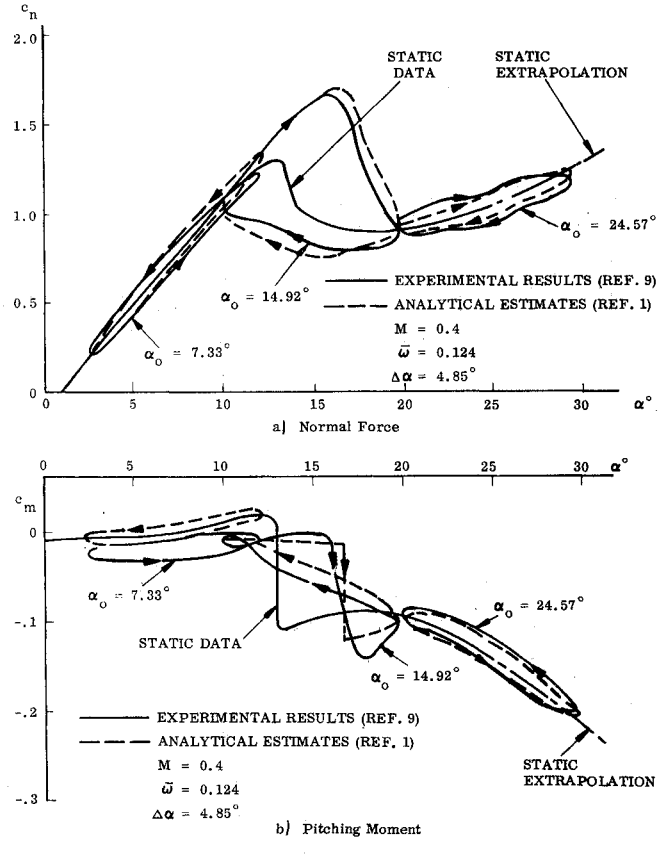

Fig. 4 Effect of angle of attack on dynamic characteristics (VERTOL 23010-1.58 airfoil section).

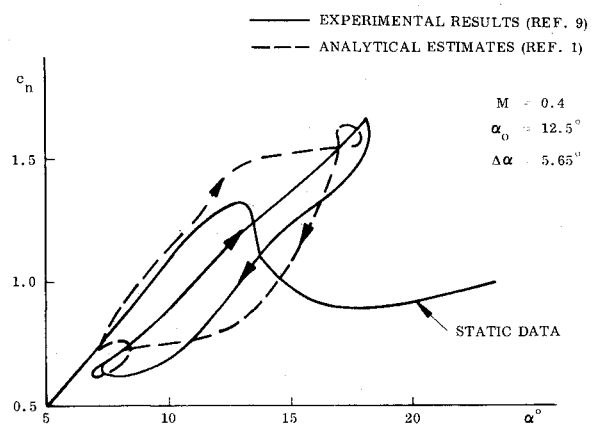

Fig. 5 Dynamic characteristics at high frequency ($\bar{\omega}$ = 0.71; VERTOL 23010-1.58 airfoil section).

with $y_0/c = 0.019$ is a prime candidate for this transition between stall types. Thus, it takes only 2% camber to cause the change from leading-edge (LE) to trailing-edge (TE) stall[5] (Fig. 2). Likewise, flight tests indicate that the stall type changes from mixed LE-TE stall to pure TE stall when stall is achieved through an abrupt pull-up maneuver.[6] In this case, the wing (NACA 66, 2X-216 tip and 66, 2X-116 root) is also a prime candidate for a pitch rate induced change in stall type with $y_0/c \approx 0.018$ at a flight Reynolds number of 14×10^6 (Fig. 1).

Figure 1 shows that, whereas the change between LE and TE type stall is rather insensitive to Reynolds number, the change from thin airfoil stall to leading-edge stall is very sensitive. Halfman's data[7] for the "sharp wing," with y_0/c = 0.013 (Fig. 3a), shows that the oscillating airfoil "generates turbulence" or in some other manner increases the effective Reynolds number enough to change the static thin airfoil stall into dynamic leading-edge stall. The oscillatory translation cannot produce any other effects peculiar only to the "sharp wing," and the time average C_L-values should agree with the static data, as they do for the "blunt wing," y_0/c = 0.022 (Fig. 3b). Figure 1 shows that the "sharp wing," y_0/c = 0.013, will be very sensitive to Reynolds number, an increase to $R_c > 2 \times 10^6$ changing the stall from thin airfoil stall (with a static $C_{L\max}$ below 1, Fig. 3a) to leading-edge stall (with $C_{L\max} > 1$, Fig. 3b). In contrast, the "blunt wing," y_0/c = 0.022, is relatively insensitive to Reynolds number changes in the range $1 < R_c \times 10^{-6} < 3$ (Fig. 1).

When the dynamic effects are not large enough to change the stall type, an analysis that in addition to the Karman-Sears vortex wake lag[8] also includes the effects of pitch rate induced flow acceleration and effective Reynolds number[1] can predict measured dynamic stall characteristics[9] using static experimental data (Fig. 4). Especially noteworthy is the

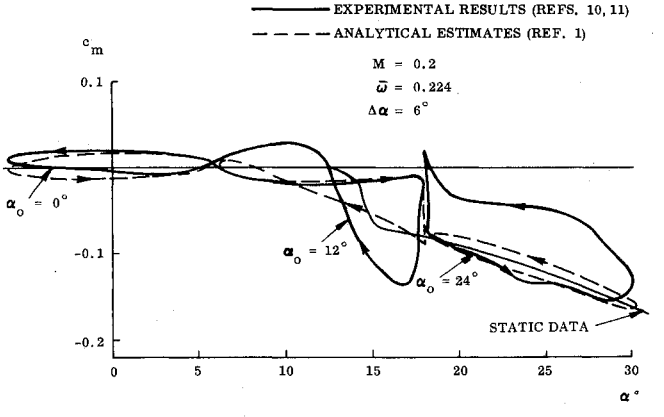

Fig. 6 Effects of angle of attack on pitching moment dynamic characteristics (NACA-0012 airfoil section).

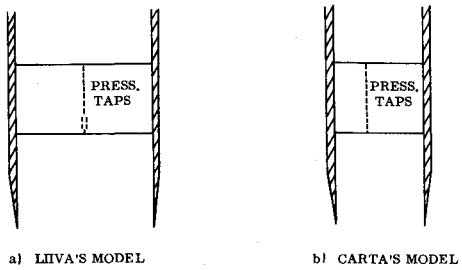

Fig. 7 Two-dimensional test geometries.

good prediction of the undamping moment loops in the stall penetration region (Fig. 4b). It is the enclosed net area that determines the damping.

The good prediction is, however, obtained only for low reduced frequencies.‡ At higher frequencies, the agreement deteriorates (Fig. 5). One likely reason is, of course, the change of stall type discussed earlier.§ Even at low frequencies, large discrepancies are sometimes observed between theoretical predictions and experimental dynamic data. Carta's low-frequency data[10,11] (Fig. 6) do not at all follow the predicted behavior. It was found that if the static reattachment characteristics were changed in a systematic manner, the experimental dynamic data could be predicted.[12] This was interpreted by the authors as a possible indication of some difficulty in simulating the dynamic stall in the wind-tunnel test. Since then¶ legitimate requests have been made for more data in support of our speculation, and such data will now be added.

As Liiva's low-frequency data[9] were predicted by our theory and Carta's[10] were not, a comparison between the experimental setups is the first logical step. They were very similar (Fig. 7). Both were using splitter plates to reduce the effects of wall boundary layer. However, one significant difference is that the Liiva-model[13] (Fig. 7a) had twice the span of the Carta model[14] (Fig. 7b). In addition, Carta et al.[14] used a row of pressure orifices placed at $\frac{2}{3}$ span instead of the midspan position used by Liiva et al.[13] Thus, one can expect Carta's data to deviate more from the two-dimensional characteristics assumed in our analysis than Liiva's data.

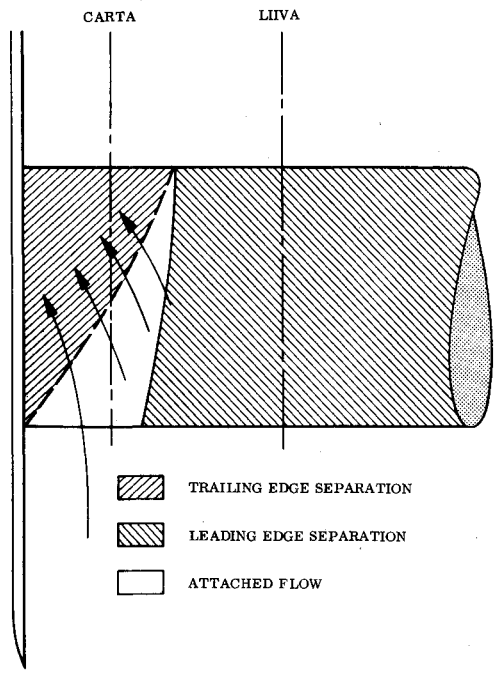

Fig. 8 Separated flow wall boundary-layer interaction.

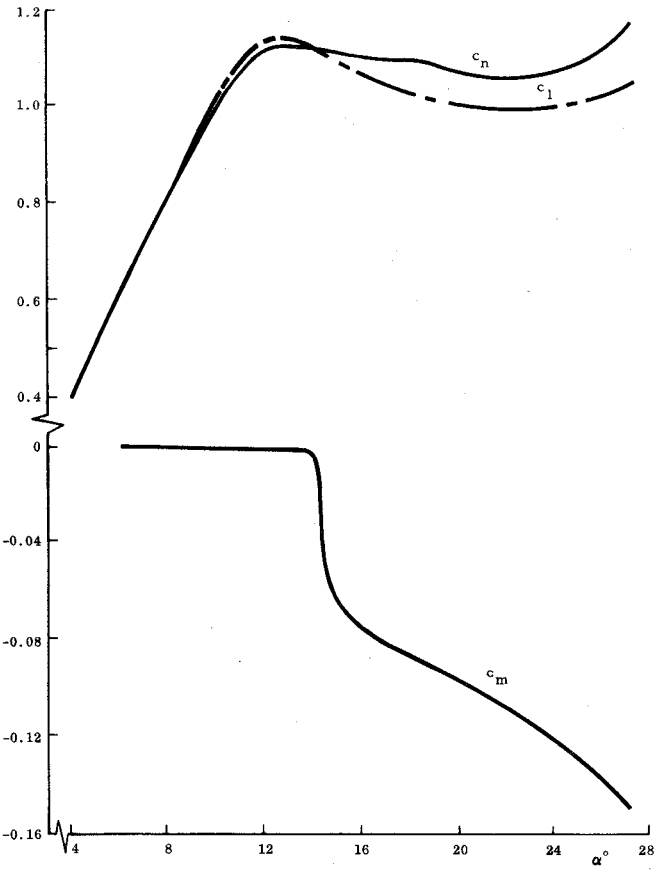

Fig. 9 NACA-0012 airfoil characteristics measured by Carta et al. at $R_c \approx 3.4 \times 10^6$.

The interaction between splitter plate boundary layer and stalled airfoil flow is likely to introduce secondary (non-two-dimensional) flow effects. It has been found that the shock induced separation on moderately thick airfoils is not truly two dimensional. The interaction between wind-tunnel wall and wing boundary layers generates vortices that have a profound effect on the pressure distribution. The stalled airfoil flow can be expected to experience similar secondary-

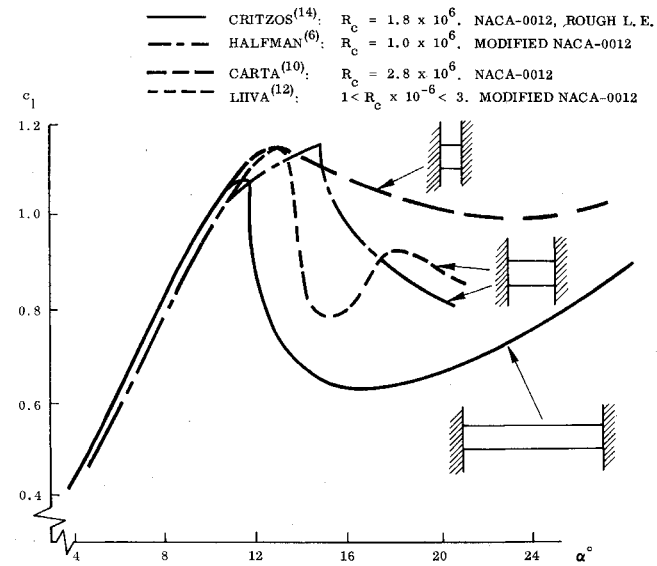

Fig. 10 Two-dimensional stall of the NACA-0012 airfoil measured by various investigators.

‡ $\bar{\omega}^2 \ll 1 : \bar{\omega} = \omega c/U$.

§ The theory assumes that the stall type does not change.

¶ AIAA Guidance, Control and Flight Mechanics Conference, Santa Barbara, Calif., August 17–19, 1970.

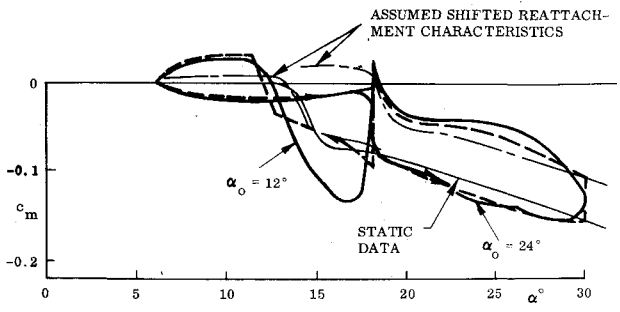

Fig. 11 Prediction of NACA-0012 dynamic characteristics using adjusted reattachment characteristics.

flow effects, and it is reasonable to suspect that the induced spanwise flow could generate pockets of trailing-edge stall near the splitter plates, as is sketched in Fig. 8. Based upon the observed effects of wing root trailing-edge stall on the stalling behavior of the straight winged space shuttle vehicle one could speculate further that the trailing-edge separation pocket will supply enough venting of the adjacent wing area to produce the patch of attached flow shown in Fig. 8 to separate the regions of leading-edge and trailing-edge stall. The different locations of the pressure orifices in the two tests could then make a great deal of difference, i.e., Liiva could measure leading-edge stall characteristics** while Carta measures trailing-edge stall (Fig. 8).

Examining the static airfoil characteristics measured by Carta et al.,[10,11,14] one finds that they are typical for trailing edge stall, with "lift stall" preceding "moment stall"[5] (Fig. 9). Comparing the lift stall characteristics measured by various investigators using two-dimensional wings,[7,11,13–15] one finds that Carta's trailing-edge type stall characteristics deviate markedly from the leading-edge type stall measured by other investigators (Fig. 10). The insets show the two-dimensional test geometries (with allowance made for the off-center location of pressure orifices on Carta's model).

Having added this information, we now reintroduce our modification of Fig. 6, in which we use static characteristics

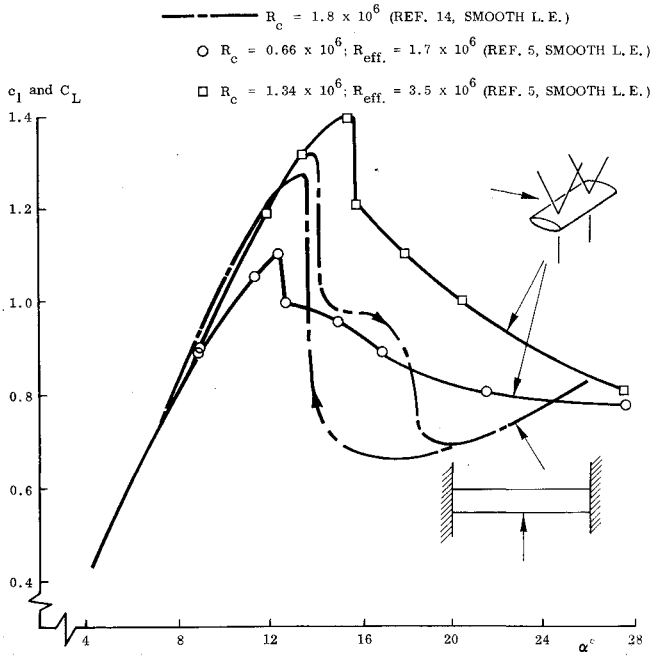

Fig. 12 NACA-0012 lift stall characteristics.

** In addition, Liiva used boundary-layer control on the end plates to eliminate any non-two-dimensional flow effects.[13]

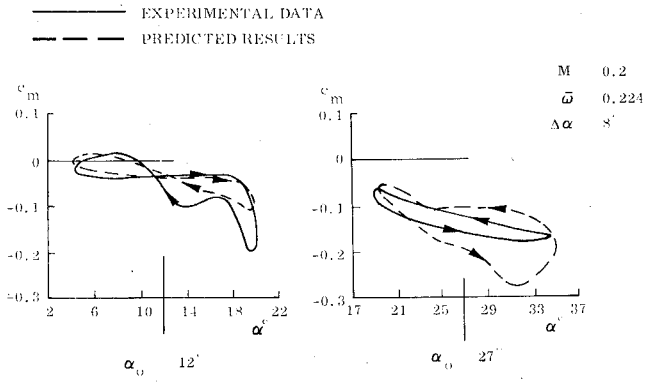

Fig. 13 Comparison between original and reconstructed dynamic pitching moment loops for NACA-0012 airfoil section oscillating around quarter chord (Ref. 11).

that have been shifted, mainly in regard to reattachment angle of attack, from the static characteristics measured by Carta (Fig. 11). The resulting agreement between theory and the measured dynamic characteristics is remarkable. Looking at the flow pattern sketched in Fig. 8, one does not find it too difficult to visualize that the boundaries for trailing edge and leading-edge stall could move in the spanwise direction for the oscillating airfoil, thereby making the "old" static characteristics inapplicable.

Even when the measuring station is several chord lengths from the splitter plates the pressure measurements can be affected by non-two-dimensional flow effects. Finite size longitudinal vortices have been observed both in "two-dimensional"[16] and "axisymmetric"[17–19] separated flow. Thus, pressure measurements at one spanwise station may not give a meaningful integrated load for the wing. In addition to the oscillatory spanwise perturbations of the pressure measurements, one has the usual concerns about variations in response characteristics for the individual pressure pickups. It appears that it is rather difficult to improve on the experimental technique used by Halfman et al.[7]††

Suppose that one is successful in obtaining truly two-dimensional dynamic stall characteristics in a sophisticated wind-tunnel test (free of the simulation difficulties discussed previously). What would be the use of these hypothetical data? For all practical applications, three-dimensional flow effects are present. The tip vortex of a straight wing ventilates the stall-flow region, and the deep stall characteristics‡‡ are widely different from the endplated or two-dimensional stall characteristics (Fig. 12). On a swept wing the leading-edge vortex supplies an even more drastic change of the stall characteristics.

There is one additional difficulty in using dynamic test data to predict full-scale (real life) dynamic stall characteristics; i.e., the highly nonlinear character of the airfoil stall characteristics. Even after elaborate curve fitting and data smoothening operations, Carta et al. cannot predict the original dynamic loops[11] [from which they sampled discrete data points to determine the coefficients in the prediction formula (Fig. 13)]. The reason is that the airfoil stall characteristics were assumed to be linear in the formulation of the curve fit polynomial. A direct comparison with our predictions is not possible, because at the time of our analysis[1,2] the data available in the open literature[10,20] were for 6° amplitude oscillations, and the predictions made by Carta et al.[11] are for 8° amplitude oscillations. Oscillations around the static stall angle $\alpha_0 = 12°$ should show similar dynamic stall characteristics for both amplitudes. However, in the deep stall region the 6° amplitude oscillations around $\alpha_0 = 24°$ will

†† They used a balance.

‡‡ After the usual corrections for finite aspect ratio has been applied.

have dynamic stall behavior similar to 8° amplitude data for $\alpha_0 = 27°$, rather than for $\alpha_0 = 24°$. (That gives minimum angles of attack of 18° and 19° for $\Delta\alpha = 6°$ and $\Delta\alpha = 8°$, respectively.) It appears that our predictions using applicable static data (Fig. 4) is superior to their "repredictions" of the dynamic data (Fig. 13).

In conclusions, it appears that dynamic stall is a phenomenon that is very difficult to simulate in subscale tests in ground facilities because of possible pitch rate induced changes of the stall type. A change of stall type can also occur locally due to variation of wind-tunnel wall and support interference effects with oscillatory frequency. This local effect will be a problem mainly in tests that use one row of pressure orifices to determine the two-dimensional airfoil characteristics. Even if truly two-dimensional results can be obtained, their application is questionable, since they do not include the ventilation of the separated flow region provided by the various types of vortices always present in the "real life" three-dimensional flowfield.

References

[1] Ericsson, L. E. and Reding, J. P., "Unsteady Airfoil Stall, Review and Extension," AIAA Paper 70-77, New York, 1970.

[2] Ericsson, L. E. and Reding, J. P., "Unsteady Airfoil Stall," LMSC Rept. N-1F-69-1, Contract NAS 1-7999, July 1969, Lockheed Missiles and Space Company, Sunnyvale, Calif.; also CR 66787, NASA.

[3] Kelly, J. A., "Effect of Modifications to the Leading-Edge Region on the Stalling Characteristics of the NACA 63_1 -012 Airfoil Section," TN 2228, 1950, NACA.

[4] Gault, D. E., "A Correlation of Low-Speed Airfoil-Section Stalling Characteristics With Reynolds Number and Airfoil Geometry," TN 3963, 1957, NACA.

[5] Jacobs, E. N. and Sherman, A., "Airfoil Section Characteristics as Affected by Variations in the Reynolds Number," TR 586, 1937, NACA.

[6] Spreiter, J. R., Galster, G. M., and Blair, W. K., "Effect of Mach and Reynolds Numbers on Maximum Lift Coefficient Obtainable in Gradual and Abrupt Stalls of a Pursuit Airplane Equipped with a Low-Drag Wing," RM A5G06, July 1945, NACA.

[7] Halfman, R. L., Johnson, H. C., and Haley, S. M., "Evaluation of High-Angle-of-Attack Aerodynamic Derivative Data and Stall-Flutter Prediction Techniques," TN 2533, 1951, NACA.

[8] Von Kármán, T. and Sears, W. R., "Airfoil Theory for Non-Uniform Motion," *Journal of Aeronautical Sciences*, Vol. 5, No. 10, Aug. 1938, pp. 379–390.

[9] Liiva, J., "Unsteady Aerodynamics and Stall Effects on Helicopter Rotor Blade Airfoil Sections," *Journal of Aircraft*, Vol. 6, No. 1, Jan.-Feb. 1969, pp. 46–51.

[10] Carta, F. O., "An Analysis of the Stall Flutter Instability of Helicopter Rotor Blades, *American Helicopter Society Journal*, Vol. 12, Oct. 1967, pp 1–18.

[11] Arcidiacono, P. J., Carta, F. O., Casellini, L. M., and Elman, H. L., "Investigation of Helicopter Control Loads Induced by Stall Flutter," USAAVLABS TR 70-2, Contract DAAJ 02-68-C-0048, March 1970, United Aircraft Corporation, Sikorsky Aircraft Division.

[12] Ericsson, L. E. and Reding, J. P., "Dynamic Stall Simulation Problems," AIAA Paper 70-945, Santa Barbara, Calif., 1970.

[13] Liiva, J., Davenport, F. J., Gray, L., and Walton, I. C., "Two-Dimensional Tests of Airfoils Oscillating Near Stall," USAAVLABS TR 68-13A & B, Contract DAAJ 02-67-C-0095, Vol. I & II, April 1968, VERTOL Div., The Boeing Co.

[14] Carta, F. O. and Niebanck, C. F., "Prediction of Rotor Instability at High Forward Speeds, Volume III, Stall Flutter," USAAVLABS TR 68-18C, Contract DA 44-177-AMC-332(T), Feb. 1969, Sikorsky Aircraft Div., United Aircraft Corp.

[15] Critzos, C. C., Heyson, H. H., and Boswinkle, R. W., Jr., "Aerodynamic Characteristics of NACA-0012 Airfoil Section at Angles of Attack from 0° to 180°," TN 3361, 1955, NACA.

[16] Ginoux, J. J., "On Some Properties of Reattaching Laminar and Transitional High Speed Flows," TN 53, 1969, Von Kármán Institute for Fluid Dynamics, Rhode-Saint-Genese, Belgium.

[17] Uebelhack, H. T., "Turbulent Flow Separation Ahead of Forward Facing Steps in Supersonic Two-Dimensional and Axisymmetric Flows," TN 54, 1969, von Kármán Institute for Fluid Dynamics, Rhode-Saint-Genese, Belgium.

[18] Reding, J. P., Guenther, R. A., Ericsson, L. E., and Leff, A. D., "Nonexistence of Axisymmetric Separated Flow," *AIAA Journal*, Vol. 7, No. 7, July 1969, pp. 1374, 1375.

[19] Ericsson, L. E., Reding, J. P., and Guenther, R. A., "Analytic Difficulties in Predicting Dynamic Effects of Separated Flow," AIAA Paper No. 70-762, Los Angeles, Calif., 1970.

[20] Carta, F. O., "Unsteady Normal Force in a Periodically Stalled Inlet Flow," *Journal of Aircraft*, Vol. 4, No. 5, Sept.-Oct. 1967, pp. 416–421.

Reduction of Tractor-Trailer Cross-Wind Response

ROGER J. HAWKS*

University of Maryland, College Park, Md.

IT has long been recognized that automobiles towing trailers are highly responsive to cross-wind disturbances. With the increasing numbers of travel trailers and camper trailers on the highways it is necessary to examine this problem to determine the effect of various parameters on the gust response.

For the purposes of this analysis the motion of an articulated automotive vehicle can be described by the three-degrees-of-freedom of lateral velocity (represented by the side-slip angle β), turn rate r, and the angle between the tractor and the trailer θ (Fig. 1). The possibility of both the tractor and the trailer rolling on the suspension is not included, thereby eliminating any effects of the vertical gradient of the cross-wind gust. Even though the vertical gradients of the wind play a large role in gust response[1]; the complication of two additional degrees of freedom makes their inclusion undesirable at this time.

The linearized equations of motion are obtained using the standard small disturbance approximations. The tire forces and moments enter the equations through the chassis stability derivatives which depend on the properties of the pneumatic tires (cornering power and aligning torque) and the mass distribution of the vehicle. The only longitudinal force which appears in the linearized equations of motion is evaluated in the reference state. Thus, if the vehicle is operated at constant speed, the longitudinal component of the wind will

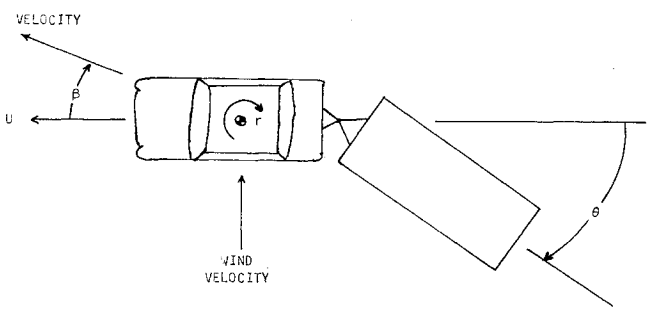

Fig. 1 Vehicle coordinates.

Presented as Paper 71-54 at the AIAA 9th Aerospace Sciences Meeting, New York, January 25–27, 1971; submitted February 3, 1971; revision received April 9, 1971.

Index Category: Aerospace Technology Utilization.

* Instructor, Department of Mechanical Engineering. Associate Member AIAA.